Proceedings of the 17th World Congress
The International Federation of Automatic Control
Seoul, Korea, July 6-11, 2008

Jet-Scheduling Control for SpiderCrane: Experimental Results

Davide Buccieri [*,1] **Christophe Salzmann** [*]
Philippe Mullhaupt [*] **Dominique Bonvin** [*]

[*] *Laboratoire d'Automatique*
École Polytechnique Fédérale de Lausanne, Switzerland

Abstract: SpiderCrane is a three-dimensional crane, whose main particularity lies in the absence of large inertial moving parts. This paper presents experimental results obtained with the novel jet-scheduling control methodology that is based on differential flatness. Jet scheduling consists essentially in using measurements to regenerate the derivatives associated with a reference trajectory. Through this regeneration, the feedforward control law, which is computed from the reference trajectory using the flatness property, is transformed into a feedback control law. Jet-scheduling control takes full advantage of the dynamic possibilities of SpiderCrane as it allows operation far away from the quasi-static mode of operation. In contrast to proportional-like compensators, the proposed control scheme does not over-react whenever the load is displaced in a persistent way, mainly because only higher derivatives are scheduled. Furthermore, the position of the upper pulley can be adapted without requiring a change in the load position, that is, without over-pulling the main cable. This general compliance makes the control methodology "user friendly" without cutting down on dynamic performance. Both point stabilization and trajectory tracking can be implemented.

Keywords: Differential flatness, Crane control, Underactuated mechanical systems, Tracking, Stabilization.

1. INTRODUCTION

Crane control has been addressed by many researchers through various methodologies, for example Corriga et al. (1998), Gustafsson (1996), Fang et al. (2003), Yoshida and Kawabe (1992), Sakawa and Sano (1997), Overton (1996), Lee et al. (2006), Yang and O'Connor (2006), Zhang et al. (2005). Linear classical designs such as LQR, although locally guaranteeing stability and performance, cannot be extended over a very large domain, mainly because of the intrinsic nonlinearities (Corriga et al. (1998), Gustafsson (1996)). These nonlinearities are essentially due to the gyroscopical coupling such as centrifugal force and centripetal acceleration (Kiss et al. (1999), Fang et al. (2003)) and to variations associated with the cable length, i.e. the natural pendulum frequency changes with cable length. Hence, passivity-based design (Fang et al. (2003), Kiss et al. (2000)) and geometrical approaches (Kiss et al. (2001), Kiss et al. (1999)) have been introduced to operate the crane over a wider domain and possibly away from the quasi-static mode (Kiss et al. (2001)).

Most crane operators move the load with the cable almost vertical; only very few of them, probably skilled through many hours of practice, venture to shift the upper trolley in anticipation of the swing and the desired final load position. To a certain extent, they avail themselves of the crane model based on their observation and experience.

This paper presents a control design methodology tailored — without real loss of generality — to SpiderCrane, allowing fully automated and efficient load positioning. Truly dynamic load displacement can be implemented through meticulous exploitation of the dynamic couplings within the mathematical model.

SpiderCrane can also be considered as a wire-driven manipulator. Normally, classical driven manipulators such as those described in (Choe et al. (1996)) and (Kawamura et al. (1995)) are designed so that there are as many actuators as degrees of freedom. However, SpiderCrane is underactuated since both angles specifying the orientation of the payload cable are not actuated, which is the main property shared with all cranes. Nevertheless, the Jet Scheduling methodology could also enrich the field of fully actuated wire-driven manipulators, especially whenever the elasticity becomes the main bottleneck in achieving high-precision positioning (Kawamura et al. (1995)). Indeed, because a pendulum is analogous to a mass-spring system, the elasticity introduces, in a certain sense, an un-actuated coordinate. Therefore, the Jet-Scheduling method could be applied to improve the positioning.

Classically, the flatness property ensures the construction of a feedforward input based on a planned motion of the flat outputs by simply combining values of the flat outputs and their time derivatives, i.e. without having to integrate differential equations (Fliess et al. (1995), Fliess et al. (1999), Kiss et al. (1999)). Therefore, in the absence of disturbances, this mechanism is sufficient to move the system from one state to another, once a trajectory compatible with the initial and final positions is designed. However, if the system has some unmodeled

[1] Supported by Swiss NSF grant number 510.524.

dynamics, an additional mechanism must be provided to make sure that the planned trajectory is indeed tracked accurately.

The point of view adopted in this paper is that, instead of specifying a trajectory and tracking it explicitly, a dynamical system called "jet scheduler" provides the derivatives (the jets) of an ideal stabilizing trajectory. These jets are updated regularly according to measurements so as to react to unknown disturbances. The proposed controller can be seen as an extension of Kiss et al. (2001) that achieves a wider domain of attraction at the cost of requiring full-state measurement.

SpiderCrane, its mathematical model, and its flatness property are presented in Section 1.1. Section 2 introduces the three parts of the jet-scheduling control methodology. Section 3 presents and discusses the experimental results that are all based on real-time experiments. Both stabilization and tracking properties are illustrated. Remarks concerning the application of Jet-Scheduling control to real cranes are given in Section 4. Finally, conclusions are given in Section 5.

1.1 SpiderCrane Setup

SpiderCrane is laboratory-scale crane design whose main particularity lies in the absence of heavy mobile components (Buccieri et al. (2005)). As a result, SpiderCrane can work at a considerably high pace, which makes it particularly useful as a laboratory setup to test advanced control laws. A slight modification of the setup described in Buccieri et al. (2005) has recently been built in the Automatic Control Laboratory of EPFL (see Figure 1). The main difference between the two designs lies in the absence of the fourth pylon (the one guiding the hosting cable). Instead, the three secondary cables are directly attached to the ring so that the load can be hoisted and lowered lowered through a combination of the three cable lengths that can be adjusted through the motor positions. The length of the main cable between the ring and the load is fixed. A short description of the setup is given next.

1.1.0.1. Setup description SpiderCrane is made of three fixed pylons. A pulley is mounted at the top of each pylon, allowing the cable to slide. The three cables are attached to a ring, and by varying their length, the ring can be moved in the surrounding space. A main cable goes through the centre of the ring and is attached to the load. The positioning of the load in space is done by adjusting the position of the ring. The position of the load of mass m is given by (x_1, x_2, x_3), that of the ring of mass m_0 by (x_{01}, x_{02}, x_{03}). The positions of the three motors are (x_{11}, x_{12}, x_{13}), (x_{21}, x_{22}, x_{23}) and (x_{31}, x_{32}, x_{33}), respectively. Furthermore, the motor inertias are considered to be equivalent to the masses m_1, m_2 and m_3, respectively, suspended to the cables. The length of the cable connecting the ring to the load is L_0. The geometrical and inertial values of SpiderCrane are given in Table 1.

The cables to the ring of length L_1, L_2 and L_3 are controlled by means of DC motors equipped with encoders, making it possible to measure the length as well as the speed of the cables. The load position (x_1, x_2, x_3) is measured through a sensor consisting of three linear cameras. The position of an infrared LED positioned on the load can be reconstructed with a precision smaller than 1 [mm].

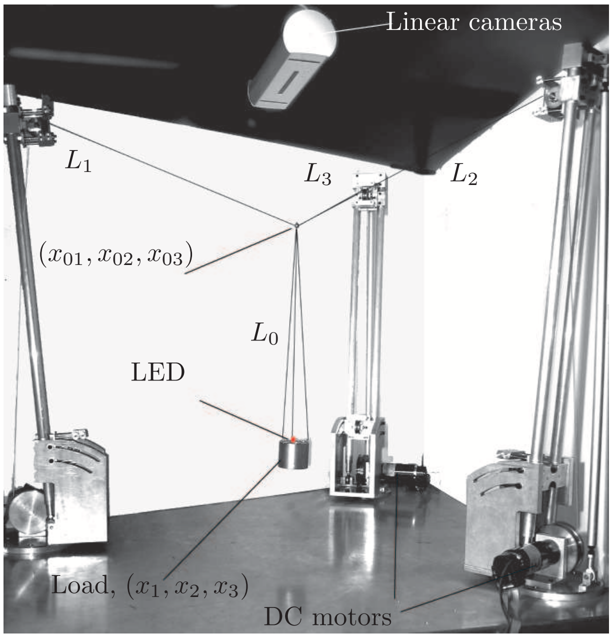

Fig. 1. Experimental setup with the three winching motors, the load with the LED, the ring, and the linear cameras.

Param.	Values	Param.	Values	Param.	Values
x_{11}	0[m]	x_{12}	0[m]	x_{13}	0[m]
x_{21}	−0.36[m]	x_{22}	0.64[m]	x_{23}	0[m]
x_{31}	0.36[m]	x_{32}	0.64[m]	x_{33}	0[m]
L_0	0.34[m]	m	0.49[kg]	m_0	0.02[kg]
m_1	0.54[kg]	m_2	0.54[kg]	m_3	0.54[kg]

Table 1. Geometrical and inertial values of SpiderCrane

The measurement readings, the control law, and the voltages applied to the motors are handled by a real-time kernel implemented in C. The control loop runs at 100 Hz. The user interface that exchanges information between the user and the real-time kernel is implemented in LabVIEW. For the interested readers, all the implementation details regarding the real-time kernel can be found in Salzmann et al. (2000).

1.2 Dynamic model

The mathematical model of SpiderCrane is derived using tools of analytical mechanics. A set q of coordinates are defined, the cardinality of which exceeds the minimal number of required generalized coordinates:

$$q = (x_1, x_2, x_3, x_{01}, x_{02}, x_{03}, L_1, L_2, L_3).$$

This set of coordinates is constrained by a set of holonomic constraints:

$$C_1 = \sum_{i=1}^{3} (x_i - x_{0i})^2 - (L_0)^2 = 0 \tag{1}$$

$$C_{j+1} = \sum_{i=1}^{3} (x_{0i} - x_{ji})^2 - L_j^2 = 0 \quad j = 1, ..., 3 \tag{2}$$

describing the geometrical relationship between the position of the crane components and the length of the cables. The external forces acting in the directions associated with the variables q are given by the three motors:

$$F_{ext} = (0, 0, 0, 0, 0, 0, T_1, T_2, T_3)$$

The Lagrange method of analytical mechanics is applied, and suitable Lagrange multipliers are introduced to handle the constraints (Greenwood (1977)). For SpiderCrane, this yields:

$$m\ddot{x}_1 = (x_1 - x_{01})\lambda_1, \tag{3}$$
$$m\ddot{x}_2 = (x_2 - x_{02})\lambda_1, \tag{4}$$
$$m\ddot{x}_3 = (x_3 - x_{03})\lambda_1 - gm, \tag{5}$$
$$\begin{aligned} m_0\ddot{x_{01}} = &(x_{01} - x_1)\lambda_1 + (x_{01} - x_{11})\lambda_2 + \\ &(x_{01} - x_{21})\lambda_3 + (x_{01} - x_{31})\lambda_4 + \end{aligned} \tag{6}$$
$$\begin{aligned} m_0\ddot{x_{02}} = &(x_{02} - x_2)\lambda_1 + (x_{02} - x_{12})\lambda_2 + \\ &(x_{02} - x_{22})\lambda_3 + (x_{02} - x_{32})\lambda_4 \end{aligned} \tag{7}$$
$$\begin{aligned} m_0\ddot{x_{03}} = &(x_{03} - x_3)\lambda_1 + (x_{03} - x_{13})\lambda_2 + \\ &(x_{03} - x_{23})\lambda_3 + (x_{03} - x_{33})\lambda_4 - gm_0, \end{aligned} \tag{8}$$
$$m_1\ddot{L_1} = T_1 - L_1\lambda_2 - L_0 \tag{9}$$
$$m_2\ddot{L_2} = T_2 - L_2\lambda_3 - L_0 \tag{10}$$
$$m_3\ddot{L_3} = T_3 - L_3\lambda_4 - L_0 \tag{11}$$

where λ_j with $j = 1, ..., 4$ are the Lagrange multipliers.

These equations, together with (1)-(2), result in a set of differential-algebraic equations (DAE) describing the dynamics. Standard integration techniques can be used (Gear and Petzold (1984)). Here, however, it is sufficient to express the Lagrange multipliers with the help of the holonomic constraints: Differentiating the constraints twice and introducing the dynamic equations results in an expression that can be solved for the Lagrange multipliers. If the initial conditions satisfy the constraints, and in the absence of numerical drift, the conditions remain satisfied throughout the simulation. However, care should be taken here not to allow large time steps. That is, either some constraint-enforcing mechanism or more involved integration technique should be considered.

1.3 Flatness of SpiderCrane

As shown in Buccieri et al. (2005), SpiderCrane is a flat system. This property is useful for computing the open-loop inputs to transfer the load from one equilibrium point to another, or to track a reference trajectory. Jet-scheduling control is a feedback law that is based on the regeneration of derivatives appearing in the correspondence between the flat outputs and the original states and inputs. For this reason, a brief reminder of the definition of flatness and an intuitive explanation of why SpiderCrane is flat is given next.

Definition 1. A system $\dot{x} = f(x, u)$ with $u \in \mathbb{R}^m$ and $x \in \mathbb{R}^n$ is said to be flat if there exists an output $y \in \mathbb{R}^m$ such that:

- the components of y are independent;
- x and u can be expressed as functions of y and its derivatives up to the r-th order

$$x = \varphi_x(y, ..., y^{(r-1)}) \quad u = \varphi_u(y, ..., y^{(r)}) \quad r \in \mathbb{N}$$

with φ_x and φ_u satisfying identically $\dot{\varphi_x} = f(\varphi_x, \varphi_u)$

Now, if the flat output describes a specific trajectory, the states and inputs will automatically follow corresponding trajectories. This is extremely useful for designing a feed-forward controller.

The choice of the flat output y and the explicit calculation of the function φ_x and φ_u are usually not trivial. In the case of SpiderCrane, one has:

$$\begin{aligned} x = &(x_1, x_2, x_3, x_{01}, x_{02}, x_{03}, L_1, L_2, L_3 \\ &\dot{x_1}, \dot{x_2}, \dot{x_3}, \dot{x_{01}}, \dot{x_{02}}, \dot{x_{03}}, \dot{L_1}, \dot{L_2}, \dot{L_3}) \\ y = &(x_1, x_2, x_3) \\ u = &(T_1, T_2, T_3) \end{aligned}$$

Using (3), (4) and (5), x_{01}, x_{02} and λ_1 can be expressed as:

$$\begin{aligned} x_{01} &= x_1 - \frac{m\ddot{x}_1}{\lambda_1} \\ &= \varphi_{x_1}(x_1, \ddot{x}_1) \end{aligned} \tag{12}$$
$$\begin{aligned} x_{02} &= x_2 - \frac{m\ddot{x}_2}{\lambda_2} \\ &= \varphi_{x_2}(x_2, \ddot{x}_2) \end{aligned} \tag{13}$$
$$\begin{aligned} \lambda_1 &= \frac{m\ddot{x}_3 + gm}{x_3 - x_{03}} \\ &= \varphi_{\lambda_1}(x_3, x_{03}, \ddot{x}_3) \end{aligned} \tag{14}$$

Differentiating (12) and (13) gives:

$$\dot{x}_{01} = \varphi_{\dot{x}_1}(x_1, \dot{x}_1, ..., x_1^{(3)}) \tag{15}$$
$$\dot{x}_{02} = \varphi_{\dot{x}_2}(x_2, \dot{x}_2, ..., x_3^{(3)}) \tag{16}$$

Solving the constraint equations (1)-(2) for L_j with $j = 1, ..., 3$, and using (12) and (13), leads to:

$$L_j = \varphi_{L_j}(x_1, \ddot{x}_1, x_2, \ddot{x}_2, x_3, \ddot{x}_3) \quad j = 1, ..., 3 \tag{17}$$

Time differentiation of (17) gives:

$$\dot{L}_j = \varphi_{\dot{L}_j}(x_1, ..., x_1^{(3)}, x_2, ..., x_2^{(3)}, x_3, ..., x_3^{(3)}) \quad j = 1, ..., 3. \tag{18}$$

Equations (12)-(18) establish that the states can be expressed as functions of the flat outputs and their derivatives.
Now, it remains to express the inputs as functions of the outputs and their derivatives and, for this purpose, (15), (16) and (18) need to be differentiated with respect to time:

$$\ddot{x}_{01} = \varphi_{\ddot{x}_{01}}(x_1, \dot{x}_1, ..., x_1^{(4)}) \tag{19}$$
$$\ddot{x}_{02} = \varphi_{\ddot{x}_{02}}(x_2, \dot{x}_2, ..., x_2^{(4)}) \tag{20}$$

$$\ddot{L}_j = \varphi_{\ddot{L}_j}(x_1, ..., x_1^{(4)}, x_2, ..., x_2^{(4)}, x_3, ..., x_3^{(4)}) \quad j = 1, ..., 3 \quad (21)$$

Solving (6)-(8) for λ_2, λ_3, λ_4 and λ_5, and using (12), (13), (14), (17), (19) and (20), gives:

$$\lambda_i = \varphi_{\lambda_i}\ (x_1, ..., x_1^{(4)}, x_2, ..., x_2^{(4)}, x_3, ..., x_3^{(4)}) \quad i = 2, ..., 4 \quad (22)$$

Finally, solving (9)-(11) for T_1, T_2, T_3 and T_4, and using (14), (17), (18), (21) and (22), results in:

$$T_j = \varphi_{T_j}\ (x_1, ..., x_1^{(4)}, x_2, ..., x_2^{(4)}, x_3, ..., x_3^{(4)}) \qquad j = 1, ..., 3 \quad (23)$$

Formally, the following expressions hold:

$$\begin{aligned}
L_j &= \varphi_{L_j}(x_1, x_2, x_3, \dot{x}_1, \dot{x}_2, \dot{x}_3, \ddot{x}_1, \ddot{x}_2, \ddot{x}_3) \qquad j = 1, ..., 3 \\
\dot{L}_j &= \varphi_{\dot{L}_j}(x_1, x_2, x_3, \dot{x}_1, \dot{x}_2, \dot{x}_3, \ddot{x}_1, \ddot{x}_2, \ddot{x}_3, x_1^{(3)}, x_2^{(3)}, x_3^{(3)}) \\
&\qquad j = 1, ..., 3 \\
T_j &= \varphi_{T_j}(x_1, x_2, x_3, \dot{x}_1, \dot{x}_2, \dot{x}_3, \ddot{x}_1, \ddot{x}_2, \ddot{x}_3, ..., x_1^{(4)}, x_2^{(4)}, x_3^{(4)}) \\
&\qquad j = 1, ..., 3
\end{aligned}$$

These relationships show that there exists a correspondence between the load position (and their time derivatives) and the original inputs and states of SpiderCrane, which means that the system is indeed flat.

2. JET-SCHEDULING CONTROL

Successful implementation of feedforward control needs to consider the discrepancies between the mathematical model and the experimental setup. For SpiderCrane, the main discrepancy relates to the characteristics of the winching mechanism. Indeed, the motors are mounted on gears that introduce a large amount of dry friction that cannot easily be compensated for through feedforward control. Furthermore, flatness-based control is inappropriate to reject disturbances, e.g. sudden unpredictable forces acting either on the load or on the motors. Hence, some feedback is necessary. One is naturally led to consider dynamic feedback linearization, i.e. using endogeneous dynamic feedback (Fliess et al. (1999)). However, this technique has a few drawbacks. The first one is the need to find the dynamic extension, which complicates the controller and especially its implementation. The second, and most important one, lies in the difficulty of separating the closed-loop dynamics in two parts, one governing the motors and the other responsible for the sway and load positionning. Such a separation would allow increasing the gains for the motors without necessarily imposing a violent load reaction.

Jet-scheduling control can answer the aforementioned drawbacks (Buccieri (2007)). The basic idea is to measure the load position and its derivatives and generate appropriate references for the three cable lengths. Jet-scheduling control has three parts:

(1) The first part calculates appropriate load accelerations (the jets χ_1, χ_2 and χ_3) to reach the load reference $(x_{1ref}, x_{2ref}, x_{3ref})$. These jets are updated regularly based on the measurements of the load position (x_1, x_2, x_3) and its derivatives $(\dot{x}_1, \dot{x}_2, \dot{x}_3)$. The regeneration of the scheduled jets upon measurements introduces the element of feedback that is needed to reject disturbances. The jets are computed using the following dynamic filter:

$$\begin{aligned}
\ddot{\chi}_1 &= -k_1^4(x_1 - x_{1ref}) - 4k_1^3(\dot{x}_1 - \dot{x}_{1ref}) \\
&\quad -6k_1^2(\chi_1 - \ddot{x}_{1ref}) - 4k_1(\dot{\chi}_1 - x_{1ref}^{(3)}) + x_{1ref}^{(4)} \\
\ddot{\chi}_2 &= -k_2^4(x_2 - x_{2ref}) - 4k_2^3(\dot{x}_2 - \dot{x}_{2ref}) \\
&\quad -6k_2^2(\chi_2 - \ddot{x}_{2ref}) - 4k_2(\dot{\chi}_2 - x_{2ref}^{(3)}) + x_{2ref}^{(4)} \\
\ddot{\chi}_3 &= -k_3^4(x_3 - x_{3ref}) - 4k_3^3(\dot{x}_3 - \dot{x}_{3ref}) \\
&\quad -6k_3^2(\chi_3 - \ddot{x}_{3ref}) - 4k_3(\dot{\chi}_3 - x_{3ref}^{(3)}) + x_{3ref}^{(4)}
\end{aligned}$$

These expressions are independent of SpiderCrane dynamics. They are stabilized chain of integrators whose inputs are the load positions and velocities. The coefficients of the characteristic polynomial are chosen such that the corresponding eigenvalues are the same and equal to $\lambda = -k_i$, so as to have few design parameters.

The above expressions should not be confused with linearizing dynamic extensions.

(2) The second part uses the flatness property to compute references for the cable lengths. The acceleration and the higher derivatives in the flatness correspondences are replaced by the ideally scheduled variables χ_1, χ_2 and χ_3 and their time derivatives:

$$\begin{aligned}
\hat{L}_j &= \varphi_{L_j}(x_1, x_2, x_3, \dot{x}_1, \dot{x}_2, \dot{x}_3, \chi_1, \chi_2, \chi_3) \quad j = 1, ..., 3 \\
\hat{\dot{L}}_j &= \varphi_{\dot{L}_j}(x_1, x_2, x_3, \dot{x}_1, \dot{x}_2, \dot{x}_3, \chi_1, \chi_2, \chi_3, \dot{\chi}_1, \dot{\chi}_2, \dot{\chi}_3) \\
&\qquad j = 1, ..., 3
\end{aligned}$$

Also, direct feedforward control on the inputs can be computed in a similar manner:

$$\hat{T}_j = \varphi_{T_j}(x_1, x_2, x_3, \dot{x}_1, \dot{x}_2, \dot{x}_3, \chi_1, \chi_2, \chi_3, ..., \ddot{\chi}_1, \ddot{\chi}_2, \ddot{\chi}_3) \quad j = 1, ..., 3$$

(3) The third part consists of feedback controllers that track the computed cable lengths. High-gains PD controllers can be used to compensate the effect of dry friction and achieve a desired convergence:

$$\begin{aligned}
T_1 &= -k_{p1}(L_1 - \hat{L}_1) - k_{d1}(\dot{L}_1 - \hat{\dot{L}}_1) + \hat{T}_1 \\
T_2 &= -k_{p2}(L_2 - \hat{L}_2) - k_{d2}(\dot{L}_2 - \hat{\dot{L}}_2) + \hat{T}_2 \\
T_3 &= -k_{p3}(L_3 - \hat{L}_3) - k_{d3}(\dot{L}_3 - \hat{\dot{L}}_3) + \hat{T}_3
\end{aligned}$$

Note that in jet-scheduling control, linearity is only enforced asymptotically (Buccieri et al. (2006)).

3. SPIDER CRANE IMPLEMENTATION

3.1 Force-controlled setup

The jet-scheduling control law uses as inputs the forces T_1, T_2 and T_3 that are applied to the three cables. However the physical inputs of the SpiderCrane setup are the voltages u_1, u_2 and u_3 to the three DC motors. For this reason, a low-level control is designed to impose the desired forces.

The torque c_i provided by each DC motor is given by

$$c_i = K_{mi}\frac{u_i - K_{ni}\omega_i}{R_i}, \quad i = 1, ..., 3 \tag{24}$$

where u_i is voltage input in [V], R_i is the coil resistance in [Ω], K_{mi} is the torque constant, K_{ni} is the velocity constant and ω_i is the motor velocity. The motor characteristics are given in Table 2.

Param.	Value	Param.	Value
Power	90[W]	τ	$6 \cdot 10^{-3}$[s]
K_m	$19.4 \cdot 10^{-3}$[Nm/A]	K_n	29460[deg/Vs]

Table 2. Motor characteristics

The velocity of the cable $\dot{L}_i$ is directly proportional to the motor velocity ω trough the pulley radius r_i,

$$\dot{L}_i = r_i\omega_i. \tag{25}$$

In the same way, the force T_i is directly proportional to the torque c_i trough the pulley radius r_i,

$$T_i = c_i r_i. \tag{26}$$

Now, inverting (24) and using (25) and (26) leads to the control law:

$$u_i = \frac{T_i c_i R_i}{r_i K_{mi}} + K_{ni}\frac{\dot{L}_i}{r_i} \tag{27}$$

The voltage u_i allows pulling on the cable L_i with the force T_i. In the sequel, we will consider the forces T_i, $i = 1, ..., 3$, as the inputs to SpiderCrane.

3.2 Experimental results

In this section, experimental results for both load stabilization and trajectory tracking are presented. The numerical values of the controller parameters used for these experiments are given in Table 3.

Param.	Values	Param.	Values	Param.	Values
k_{pi}[V/m]	80	k_{di}[Vs/m]	15	k_i	8[1/s]

Table 3. Controller parameters ($i = 1, ..., 3$).

The results described next are also available in movie form [2].

Stabilization. Figure 2 illustrates the way in which the jet-scheduling controller stabilizes the load at the reference point $(x_{1ref}, x_{2ref}, x_{3ref})$. The experiment has two phases: (i) without control, the load oscillates strongly, and (ii) at time 3.5[s], the controller is switched on. The controller stabilizes nicely the load at its reference point. Moreover, the performance is excellent since the time needed for stabilization is of the order of 1.5 [s].

Figure 3 illustrates the controller behavior following a disturbance that imposes a load position different from the reference value. This corresponds to the situation where the load is being blocked by some obstacle, or a human operator pulls and holds the load away from the reference value. As can be seen by the small values of the inputs u_1, u_2, and u_3, the controller does not overreact. The controller knows that, under normal conditions,

[2] http://lawww.epfl.ch/page4506.html

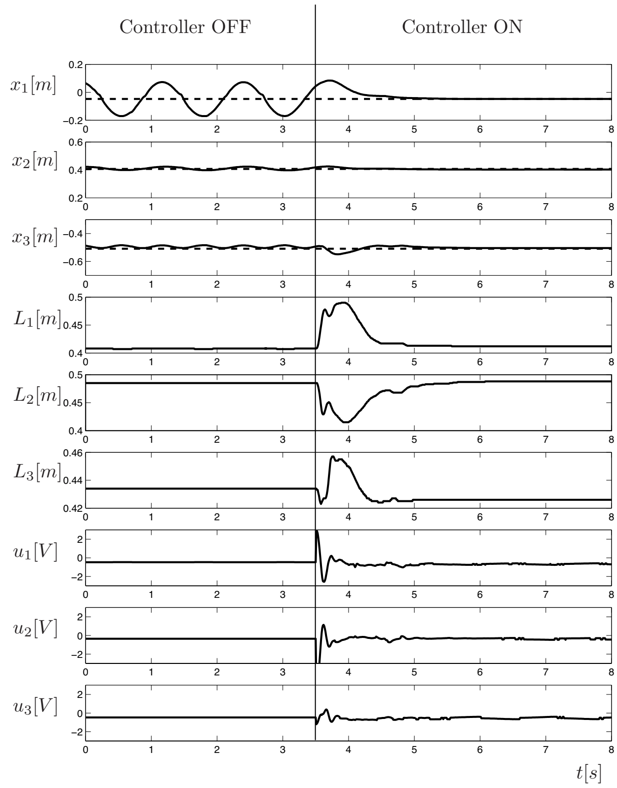

Fig. 2. Load oscillation without control and load stabilization with jet-scheduling control. Reference values are represented by dashed lines.

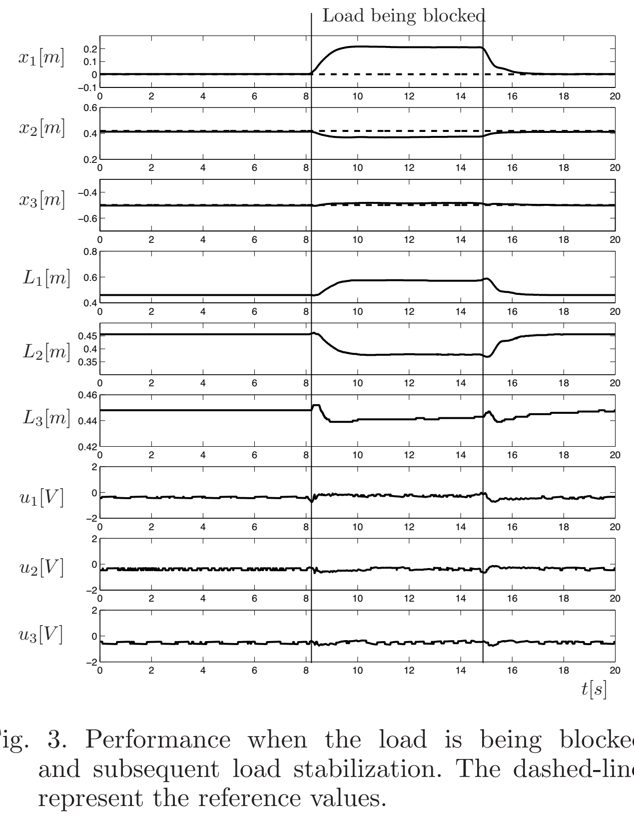

Fig. 3. Performance when the load is being blocked, and subsequent load stabilization. The dashed-lines represent the reference values.

small forces are sufficient to go back to the reference position. The fact that small forces are not able to move the load indicates the presence of an "unusual" situation. The controller, which works with higher derivatives of the position error, does not compute the large control effort that a proportional-like controller would. The figure also shows that, once the load is released, it goes back swiftly to its equilibrium position without any oscillation.

Trajectory tracking. A circular reference trajectory is provided. Figures 4 and 5 show that the load position tracks the reference even after a sudden disturbance takes place at time $t = 2.7s$. Again, the load rapidly catches up with the reference in a highly dynamic fashion. This can also be seen in the 3D Figure 5 where, once the disturbance takes place, the load rapidly cuts across the circle, along the diameter, to catch back with the reference.

Careful examination shows that there remains a slight tracking error along the x_3-axis, which is not the same for each rotation. However, the x_1 and x_2-axes are in perfect agreement with the references. This can be explained by the following geometrical consideration. Table 1 shows that the chosen ring position $x_{3ref} = -0.49[m]$ is close to that of the fixed pylons. Hence, this requires a large force along the horizontal cables, and leads to a loss of sensitivity.

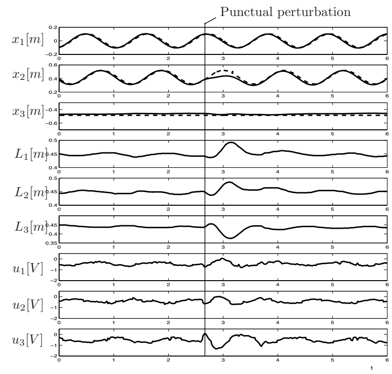

Fig. 4. Tracking of a circular reference (height $x_{3ref} = -0.49$ [m], center at $x_{1ref} = 0$ [m], $x_{2ref} = 0.41$ [m], radius 0.1 [m], frequency 0.9 [Hz]). A sudden and short perturbation is applied at time $t = 2.7$ [s]. The dashed-lines represent the reference values.

As a general remark, whenever a persistent disturbance occurs on the load (even a large one), the upper pulley quickly re-positions itself so as to bring the load back to its reference value without over-pulling the main cable. This general compliance makes the controller "user friendly" and increases the security level without performance loss.

4. APPLICATION TO REAL CRANES

Although the paper has addressed SpiderCrane control, a few remarks on how to apply the method to other types of cranes and especially real cranes. Because cranes are flat systems, as it has been shown in Kiss et al. (1999), they can be controlled using the jet-scheduling methodology. The difference lies in how the payload position is measured and how the operator specifies the flat reference trajectory.

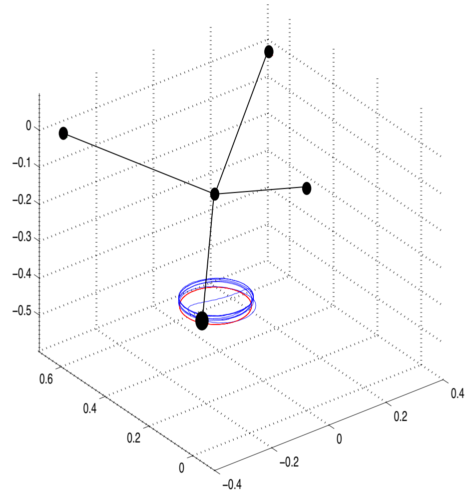

Fig. 5. Three-dimensional view of the tracking of a circular reference. The reference is in solid red.

Concerning the payload-position measurement, some real cranes are equipped with a device that mechanically measures the angle of the main cable. Together with the full measurement of the cable lengths (at the winch level), this allows restoring the payload position. Of course, a camera-like measurement device is not advisable due to possible harsh-weather conditions.

Although finding the flat output of a general nonlinear dynamical system is not an easy task, specifying a flat output trajectory — once it is known — is very simple, because the time evolution of the flat output does not have to obey any kind of differential equation. The paper presented a circular type trajectory, but a polynomial one is also possible. Additionally, one can consider the following trajectory generator, which is better adapted to human operators: Consider again SpiderCrane and only the x_1 flat output (the other outputs are treated in a similar fashion). Now, x_{1ref} $\dot{x}_{1ref}$, $\ddot{x}_{1ref}$, $x^{(3)}_{1ref}$ and $x^{(4)}_{1ref}$ are provided by the following dynamical filter:

$$x^{(4)}_{1ref} = -4k^3 x^{(4)}_{1ref} - 6k^2 x^{(4)}_{1ref} \\ -4k x^{(4)}_{1ref} + k^4 (x_{1des} - x_{1ref}) \qquad (28)$$

where d x_{1des} is the desired position specified by the operator (i.e. the input to the filter). Clearly, x_{1ref} is differentiable four times and the filter provides all the derivatives. The parameter $k > 0$ is chosen so as to generate either a slow convergence (when small) or a fast convergence (when large) to the desired position that the operator specifies.

5. CONCLUSIONS

The paper has presented the application of a novel control scheme — called jet-scheduling control — to SpiderCrane. Jet-scheduling control shows highly dynamic responses in point stabilization, disturbance rejection, and trajectory tracking. Moreover, the control scheme does not over-react when the load gets blocked.

The following characteristics of jet-scheduling control can be mentioned:

- There is no need to measure high derivatives of the flat outputs. Only the first derivatives are necessary. All higher-order derivative information is provided by the jet scheduler (the χ variables and their derivatives).
- Linearization is achieved only upon convergence.

The main enhancements of the jet-scheduling methodology over, say, classical dynamic feedback linearization, are essentially twofold. On the one hand, it allows dealing with unmodeled motor characteristics (for instance dry friction) through a natural dynamic separation between motor reference tracking (high gain) and trajectory stabilization (scheduled jets). On the other hand, the control methodology does not require the computation of the specific dynamic extension needed to fully linearize the system. The design of the controller is therefore, to a certain extent, more intuitive. A full theoretical comparison between jet-scheduling control and dynamic feedback linearization for a flat mobile robot is given in Buccieri et al. (2006).

REFERENCES

D. Buccieri. *Jet-Scheduling Control for Flat Systems*. Ecole Polytechnique Fédérale de Lausanne, 2007.

D. Buccieri, Ph. Mullhaupt, and D. Bonvin. Spider-crane: Model and properties of a fast weight-handling equipment. In *IFAC World Congress*, Prague, Czech Republic, July 2005.

D. Buccieri, Ph. Mullhaupt, Z. P. Jiang, and D. Bonvin. Velocity scheduling controller for a nonholonomic mobile robot. In *The 25th Chinese Control Conference*, Harbin, China, August 2006.

W. Choe, H. Kino, K. Katsuta, and S. Kawamura. Design of Parallel Wire Driven Robots for Ultrahigh Speed Motion Based on Stiffness Analysis. In *Japan/USA Symposium on Flexible Automation*, pages 159–166, 1996.

G. Corriga, A. Giua, and G Usai. An implicit gain-scheduling controller for cranes. *IEEE Trans. on Cont. Sys. Tech.*, 6(1):15–10, January 1998.

Y. Fang, W. E. Dixon, D. M. Dawson, and E. Zergeroglu. Nonlinear coupling control laws for an underactuated overhead crane system. *IEEE/ASME Transactions on Mechatronics*, 8(3):418–423, 2003.

M. Fliess, J. Lévine, Ph. Martin, and P. Rouchon. Flatness and defect of nonlinear systems: Introductory theory and examples. *International Journal of Control*, 61(6): 1327–1361, 1995.

M. Fliess, J. Lévine, Ph. Martin, and P. Rouchon. A Lie-Bäcklund approach to equivalence and flatness of nonlinear systems. *IEEE Transactions on Automatic Control*, 44:922–937, 1999.

C. W. Gear and L. R. Petzold. ODE methods for the solutions of differential-algebraic systems. *L. Numer. Anal.*, 21:716–728, 1984.

D. T. Greenwood. *Classical Dynamics*. Prentice-Hall, Englewood Cliffs, N.J., 1977.

T. Gustafsson. On the design and implementation of a rotary crane controller. *European J. Control*, 2(3):166–175, March 1996.

S. Kawamura, W. Choe, S. Tanaka, and Pandian S. R. Development of an Ultrahigh Speed Robot FALCON using Wire Drive System. In *IEEE International Conference on Robotics and Automation*, pages 215–220, 1995.

B. Kiss, J. Lévine, and Ph. Mullhaupt. Modelling, flatness and simulation of a class of cranes. *Periodica Polytechnica Ser. El. Eng.*, 43(3):215–225, 1999.

B. Kiss, J. Lévine, and Ph. Mullhaupt. A simple output feedback controller for nonlinear cranes. In *Proceedings of the 43rd IEEE CDC*, pages 5097–5101, Sydney, Australia, December 2000.

B. Kiss, J. Lévine, and Ph. Mullhaupt. Global stability without motion planing may be worse than local tracking. In *Proceedings of the ECC*, pages 1106–1110, Porto, Portugal, June 2001.

H.-H. Lee, Y. Liang, and D. Segura. A sliding-mode antiswing trajectory control for overhead cranes with high-speed load hoisting. *Journal of Dynamic Systems, Measurement and Control, Transactions of the ASME*, 128:842–845, 2006.

R. H. Overton. Anti-sway control system for cantilever cranes. *Unates States Patent*, (5,526,946), June 1996.

Y. Sakawa and H. Sano. Nonlinear model and linear robust control of overhead traveling cranes. *Nonlinear Analysis*, 30, December 1997.

Ch. Salzmann, D. Gillet, and P. Huguenin. Introduction to real-time control using LabVIEW with an application to distance learning. *International Journal of Engineering Educationl*, 16(3):255–272, 2000.

T.W. Yang and W.J. O'Connor. Wave based robust control of a crane system. *IEEE International Conference on Intelligent Robots and Systems, art. no. 4058803*, pages pp. 2724–2729, 2006.

K. Yoshida and H. Kawabe. A design of saturating control with a guaranteed cost and its application to the crane control system. *IEEE Transactions on Automatic Control*, 37(1):121–127, January 1992.

X. Zhang, B. Gao, and H. Chen. Nonlinear controller for a gantry crane based on partial feedback linearization. In *Proceedings of the 5th International Conference on Control and Automation, ICCA'05*, pages 1074–1078, 2005.